The 2009 IEEE/RSJ International Conference on
Intelligent Robots and Systems
October 11-15, 2009 St. Louis, USA

Efficient Parametric Excitation Walking with Delayed Feedback Control

Yuji Harata, Fumihiko Asano, Kouichi Taji and Yoji Uno

Abstract— **In the passive dynamic walking proposed by McGeer, mechanical energy lost by heel strike is restored by transporting potential energy to kinetic energy as walking down a slope. When energy input is large such as an angle of slope is steep, bifurcation of walking period occurs. In parametric excitation walking, which is one method to realize passive dynamic-like walking on level ground, bifurcation has also been observed when walking speed is fast. Recently, Asano et al. have shown that bifurcation exerts an adverse influence upon walking performance by using rimless wheel model. In this paper, we apply delayed feedback control (DFC) originally used in chaos control to parametric excitation walking to suppress bifurcation. We show in numerical simulation that the proposed method makes two-period walking to one-period walking, and energy efficiency is improved. The analyses using Poincaré map reveal that the one-period walking with DFC is unstable periodic orbit and that the robot dealt in this paper satisfies the sufficient condition of applicability of DFC.**

I. INTRODUCTION

In the dynamic walking, restoration of mechanical energy lost by heel strike is requisite for sustainable walking. In passive dynamic walking proposed by McGeer [1], potential energy is transported to kinetic energy as walking down a slope. For sustainable walking on level ground, several methods, such as energy tracking control [2], virtual passive dynamic walking [3] and so on, were proposed from the view point of restoration of mechanical energy. Among them, parametric excitation method restores mechanical energy by up-and-down movement of the center of mass, and then sustainable walking is realized on level ground [4], [5].

In passive dynamic walking, bifurcation of walking period has been observed as slope becomes large, i.e., input energy becomes large [6]. Osuka and Kirihara showed that bifurcation occurred by experiment for real biped robot [7]. Parametric excitation walking proposed by Harata et al. realizes sustainable walking on level ground with only knee torque that moves the center of mass of swing-leg up-and-down [8], [9]. It is also observed that two-period walking appears in their model when the amplitude of reference trajectory for knee angle is large. Recently, Asano et al. have shown that bifurcation exerts an adverse influence upon walking performance by using rimless wheel model [10].

Delayed feedback control (DFC) originally used in chaos control stabilizes unstable periodic orbit [11]. Osuka et al. applied DFC to passive dynamic walking [12] and showed that DFC made the biped robot more robust against disturbance.

In this paper, we apply DFC to the parametric excitation walking proposed by Harata et al. [8]. The purpose of introducing DFC is to suppress bifurcation. The proposing method designs the swing-leg knee torque by parametric excitation method and the hip torque by DFC in a similar way to Osuka et al. [12]. We numerically show that the proposed method makes two-period walking to one-period walking, and, at the same time, energy efficiency is improved. The analyses using Poincaré map reveal that the one-period walking with DFC is unstable periodic orbit and that the robot dealt in this paper satisfies the sufficient condition of applicability of DFC.

This paper is organized as follows. Section II explains the biped robot treated in this paper. In section III, we explain parametric excitation method and DFC. Section IV is the main results of this paper, in which the effect of DFC is shown by numerical simulation and the analysis using Poincaré map is presented. Finally in Section V, we conclude this paper.

II. MODEL OF PLANAR BIPED ROBOT WITH SEMICIRCULAR FEET

In this section, we explain the dynamic equation and the impact equation of the biped robot treated in this paper.

A. Dynamic equation

Fig. 1 illustrates the biped robot dealt in this paper. The robot has four point masses and three degrees of freedom, and has semicircular feet whose centers are on each leg. Since there are two mass on the leg, the support-leg has inertia moment. The dynamic equation during single support phase takes the form

$$\boldsymbol{M}(\boldsymbol{\theta})\ddot{\boldsymbol{\theta}} + \boldsymbol{C}(\boldsymbol{\theta},\dot{\boldsymbol{\theta}})\dot{\boldsymbol{\theta}} + \boldsymbol{g}(\boldsymbol{\theta}) = \boldsymbol{S}\boldsymbol{u} - \boldsymbol{J}^{\mathrm{T}}\lambda, \qquad (1)$$

where $\boldsymbol{\theta} = \begin{bmatrix} \theta_1 & \theta_2 & \theta_3 \end{bmatrix}^{\mathrm{T}}$ is the generalized coordinate vector, $\boldsymbol{M}$ is the inertia matrix, $\boldsymbol{C}$ is the Coriolis force and the centrifugal force, and $\boldsymbol{g}$ is the gravity vector. The matrix $\boldsymbol{J} = \begin{bmatrix} 0 & 1 & -1 \end{bmatrix}$ is a Jacobian derived from a knee constraint, $\theta_2 = \theta_3$, and $\lambda \in \mathbb{R}$ is knee binding force. Control input vector $\boldsymbol{S}\boldsymbol{u}$ in Eq. (1) is given by

$$\boldsymbol{S}\boldsymbol{u} = \begin{bmatrix} 1 & 0 \\ -1 & -1 \\ 0 & 1 \end{bmatrix} \begin{bmatrix} u_H \\ u_K \end{bmatrix} = \begin{bmatrix} \boldsymbol{S}_H & \boldsymbol{S}_K \end{bmatrix} \begin{bmatrix} u_H \\ u_K \end{bmatrix}, \qquad (2)$$

where u_H is the hip torque and u_K is the knee torque. In the proposed control method, knee torque u_K is used to restore

Y. Harata, K. Taji and Y. Uno are with the Department of Mechanical Science and Engineering, Graduate School of Engineering, Nagoya University, Furocho, Chikusa, Nagoya, 464-8603, Japan {y_harata, taji, uno}@nuem.nagoya-u.ac.jp

F. Asano is with the School of Information Science, Japan Advanced Institute of Science and Technology, 1-1 Asahidai, Nomi, Ishikawa 923-1292, Japan fasano@jaist.ac.jp

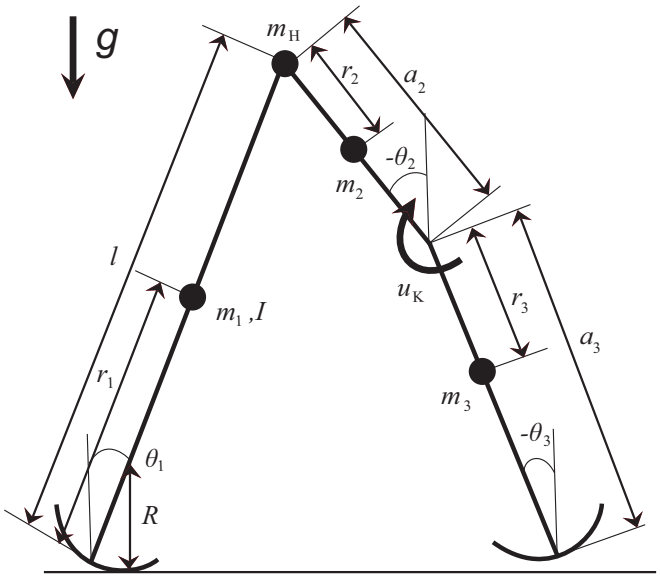

Fig. 1. Model of planar kneed biped robot with semicircular feet

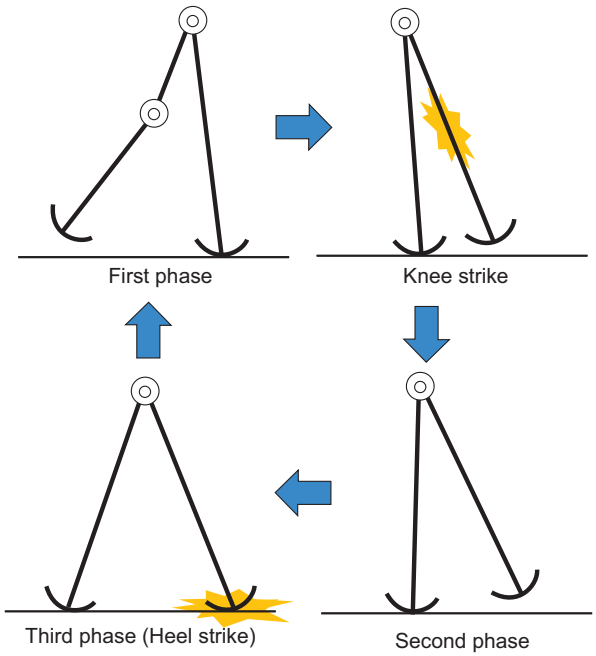

Fig. 2. Walking phases

mechanical energy by parametric excitation effect, and hip torque u_H is designed based on DFC which is used only to suppress bifurcation.

In this robot, collisions occur at a knee and at the ground. The gait of robot consists of the following three phases (Fig. 2).

- The first phase (Single support phase I): The support-leg rotates around the contact point between a semicircular foot and ground, and the knee of swing-leg is not fixed, that is, knee binding force λ equals to zero, and knee angle of swing-leg is controlled by input torque.
- The second phase (Single support phase II): The support-leg rotates around the contact point and the knee of swing-leg is locked in a straight posture by knee binding force. When the first phase changes to the second phase, a completely inelastic collision occurs at a knee.
- The third phase (Double support phase): This phase occurs instantaneously, and the support-leg and the swing-leg are exchanged after the collision at the ground.

B. Impact equation

We first explain the impact equation at a knee of swing-leg. Let the coordinates $\dot{\boldsymbol{\theta}}^-$ and $\dot{\boldsymbol{\theta}}^+$ correspond to before and after knee collision, respectively. Then these are related by the equation

$$\boldsymbol{M}\dot{\boldsymbol{\theta}}^+ = \boldsymbol{M}\dot{\boldsymbol{\theta}}^- + \boldsymbol{J}^{\mathrm{T}}\lambda_K, \tag{3}$$

where λ_K is the constraint force making $\boldsymbol{J}\dot{\boldsymbol{\theta}}^+ = 0$. This force is given by

$$\lambda_K = -(\boldsymbol{J}\boldsymbol{M}^{-1}\boldsymbol{J}^{\mathrm{T}})^{-1}\boldsymbol{J}\dot{\boldsymbol{\theta}}^-. \tag{4}$$

From Eqs. (3) and (4), angular velocities after knee collision are given by

$$\dot{\boldsymbol{\theta}}^+ = (\boldsymbol{I} - \boldsymbol{M}^{-1}\boldsymbol{J}^{\mathrm{T}}(\boldsymbol{J}\boldsymbol{M}^{-1}\boldsymbol{J}^{\mathrm{T}})^{-1}\boldsymbol{J})\dot{\boldsymbol{\theta}}^-. \tag{5}$$

We assume that, once after knee collision, a knee-joint is fixed by the force $\boldsymbol{J}^{\mathrm{T}}\lambda$ until collision at the ground occurs.

Next, we explain the impact equation at the ground. We assume also that a collision at the ground is completely inelastic. The generalized coordinate of each legs $i, (i = 1, 2)$ for separated model shown by Fig. 3 is given by

$$\boldsymbol{q} = \begin{bmatrix} \boldsymbol{q}_1 \\ \boldsymbol{q}_2 \end{bmatrix}, \tag{6}$$

where $\boldsymbol{q}_i = \begin{bmatrix} x_i & z_i & \theta_{i1} & \theta_{i2} \end{bmatrix}^{\mathrm{T}}$. Let "$-$" and "$+$" be superscripts indicating just before and just after impact at the ground, respectively. Then, we have $\boldsymbol{q}^- = \boldsymbol{q}^+$, because the positions do not change before and after impact. The impact equation of generalized coordinates takes the form

$$\bar{\boldsymbol{M}}(\boldsymbol{q})\dot{\boldsymbol{q}}^+ = \bar{\boldsymbol{M}}(\boldsymbol{q})\dot{\boldsymbol{q}}^- - \boldsymbol{J}_I(\boldsymbol{q})^{\mathrm{T}}\boldsymbol{\lambda}_I, \tag{7}$$

where $\bar{\boldsymbol{M}}$ is inertial matrix for generalized coordinates of the robot and $\boldsymbol{\lambda}_I \in \mathbb{R}^6$ is undetermined multiplier vector corresponding to impulse force and $\boldsymbol{J}_I \in \mathbb{R}^{6\times 8}$ is the Jacobian such that

$$\boldsymbol{J}_I(\boldsymbol{q})\dot{\boldsymbol{q}}^+ = \boldsymbol{0}_{6\times 1}. \tag{8}$$

There are some constraints among the coordinates. From geometric conditions, we have the following three equations,

$$\begin{aligned} & z_2 = R, \\ & x_1 + (a_3 - R)\sin\theta_{11} + a_2\sin\theta_{12} \\ & \quad = x_2 + (a_3 - R)\sin\theta_{21} + a_2\sin\theta_{22}, \\ & z_1 + (a_1 - R)\cos\theta_{11} + a_2\cos\theta_{12} \\ & \quad = z_2 + (a_1 - R)\cos\theta_{21} + a_2\cos\theta_{22}. \end{aligned} \tag{9}$$

These equations mean that z-position of central point of foot is equal to foot radius and that vertical and horizontal

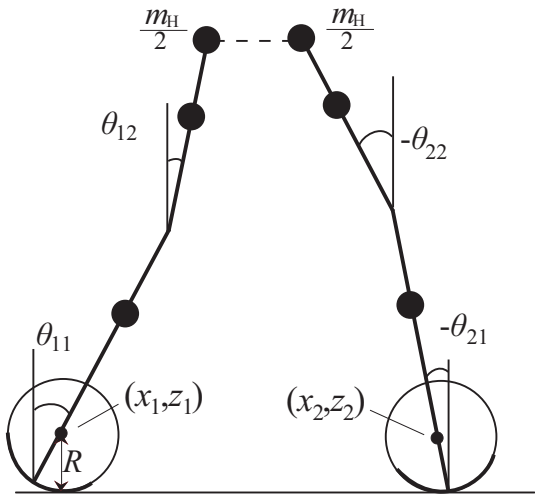

Fig. 3. Generalized coordinates at the heel-strike instant

hip positions from (x_1, z_1) equal to those from (x_2, z_2). In addition, the rate constraint, that is, a foot of support-leg rolls on the ground without slip, is given by

$$\dot{x}_2^+ = R\dot{\theta}_{21}^+. \tag{10}$$

The rate constraints that knees are fixed in a straight posture are given by

$$\dot{\theta}_{11}^+ = \dot{\theta}_{12}^+,\ \dot{\theta}_{21}^+ = \dot{\theta}_{22}^+. \tag{11}$$

The Jacobian $\boldsymbol{J}_I$ is derived by differentiating Eq. (9) and by incorporating Eqs. (10) and (11).

The multiplier vector $\boldsymbol{\lambda}_I$ is given by

$$\boldsymbol{\lambda}_I = (\boldsymbol{J}_I \bar{\boldsymbol{M}}^{-1} \boldsymbol{J}_I^{\mathrm{T}})^{-1} \boldsymbol{J}_I \dot{\boldsymbol{q}}^-. \tag{12}$$

By substituting Eq. (12) into Eq. (7), the velocity of generalized coordinate after collision becomes

$$\dot{\boldsymbol{q}}^+ = (\boldsymbol{I}_8 - \bar{\boldsymbol{M}}^{-1} \boldsymbol{J}_I^{\mathrm{T}} \boldsymbol{X}_I^{-1} \boldsymbol{J}_I) \dot{\boldsymbol{q}}^-. \tag{13}$$

III. CONTROL INPUT DESIGN

In this section, we design the control input for swing-leg knee based on parametric excitation method and that for hip based on DFC.

A. Parametric excitation walking

In this subsection, we explain the parametric excitation walking with knees [8]. In a parametric excitation method, up-and-down motion of the center of mass restores mechanical energy lost by heel strike. In our model, up-and-down motion is realized by bending and stretching a swing-leg knee. Then, sustainable walking can be generated by controlling a knee angle appropriately. We give the reference trajectory h, shown by

$$\begin{aligned} h(t) &= (\theta_2 - \theta_3)_d \\ &= \begin{cases} A_m \sin^3\left(\frac{\pi}{T_{\mathrm{set}} - \delta}(t - \delta)\right) & (\delta \le t \le T_{\mathrm{set}}), \\ 0 & (\text{otherwise}), \end{cases} \end{aligned} \tag{14}$$

where $\delta > 0$ is the bending delay, A_m is the desired amplitude of vibration and T_{set} is the desired settling-time which is the period during bending and stretching a knee. Fig. 4 illustrates an example of reference trajectory where $A_m = 0.8$rad, $T_{set} = 0.8$s and $\delta = 0.2$s. We note that, in the trajectory h, the angular velocity equals to zero when the beginning of bending and the end of stretching a knee, and hence, the collision at knee is almost negligible.

We can make swing-leg knee angle to track the reference trajectory with partial feedback linearization method [8], and the control input to track the reference trajectory h is given by

$$\begin{aligned} u_K = &\left(\begin{bmatrix} 0 & 1 & -1 \end{bmatrix} \boldsymbol{M}^{-1} \boldsymbol{S}_K\right)^{-1} \begin{bmatrix} 0 & 1 & -1 \end{bmatrix} \boldsymbol{M}^{-1} \\ &\times \left(\boldsymbol{M} \begin{bmatrix} 0 & 0 & -\ddot{h} \end{bmatrix} + \boldsymbol{C}\dot{\boldsymbol{\theta}} + \boldsymbol{g} - \boldsymbol{S}_H u_H\right). \end{aligned} \tag{15}$$

We note that the reference trajectory is traced completely even if additional hip torque exists.

B. Delayed feedback control (DFC)

In this subsection, we explain DFC, which originally used in chaos control to stabilize unstable periodic orbit [11].

Let define $\boldsymbol{x}(k)$ be states of a discrete dynamical system defined by

$$\begin{aligned} \boldsymbol{x}(k+1) &= \mathcal{F}(\boldsymbol{x}(k), \boldsymbol{u}(k)), \\ \boldsymbol{y}(k) &= \mathcal{G}(\boldsymbol{x}(k)), \end{aligned} \tag{16}$$

where $\mathcal{F}$ is a mapping, $\mathcal{G}$ is an output function for observed value $\boldsymbol{y}(k)$ and $\boldsymbol{u}(k)$ is an input.

Let also $\boldsymbol{x}^*$ be an equilibrium of the discrete dynamical system Eq. (16). Then, by linearizing the system around the equilibrium $\boldsymbol{x}^*$, we obtain

$$\begin{aligned} \delta\boldsymbol{x} &= \boldsymbol{A}\delta\boldsymbol{x} + \boldsymbol{B}\boldsymbol{u} \\ \boldsymbol{y} &= \boldsymbol{C}\boldsymbol{x}, \end{aligned} \tag{17}$$

where $\delta\boldsymbol{x} = \boldsymbol{x} - \boldsymbol{x}^*$ and

$$\begin{aligned} &\boldsymbol{A} = \tfrac{\partial}{\partial \boldsymbol{x}} \mathcal{F}(\boldsymbol{x}^*, 0), \qquad \boldsymbol{B} = \tfrac{\partial}{\partial \boldsymbol{u}} \mathcal{F}(\boldsymbol{x}^*, 0), \\ &\boldsymbol{C} = \tfrac{\partial}{\partial \boldsymbol{x}} \mathcal{G}(\boldsymbol{x}^*, 0). \end{aligned} \tag{18}$$

It has been shown in [12] that if the inequality

$$\det(\boldsymbol{I}_n - \boldsymbol{A}) > 0 \tag{19}$$

holds, there is a feedback gain $\boldsymbol{K}$ such that the DFC input torque $\boldsymbol{u}(k)$ defined by

$$\boldsymbol{u}(k) = \boldsymbol{K}(\boldsymbol{y}(k-1) - \boldsymbol{y}(k-2)) \tag{20}$$

stabilizes the *unstable* equilibrium $\boldsymbol{x}^*$. We will show in subsection IV-C that the condition Eq. (19) holds for our biped model.

In biped walking, it is natural to take the generalized coordinate just after heel strike of k-th step as the state $\boldsymbol{x}(k)$ of the discrete dynamical system Eq. (16). Then, the mapping $\mathcal{F}$ is considered to output the next states $x(k+1)$ just after heel strike of $(k+1)$-th step when the control input $u(k)$ during $(k+1)$-th step exists. This mapping can be derived by integration and calculation of Eqs. (1), (5) and (13). We note

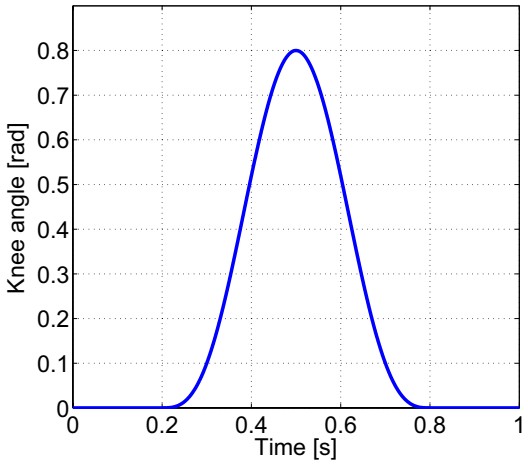

Fig. 4. Reference trajectory for knee angle

TABLE I
PHYSICAL PARAMETERS OF THE KNEED BIPED ROBOT

r_1	0.40	m	R	0.575	m
r_2	0.20	m	m_1	5.0	kg
r_3	0.30	m	m_2	1.0	kg
a_2	0.40	m	m_3	4.0	kg
a_3	0.60	m	m_H	5.5	kg
l	1.0	m	I	2.0	kg $\cdot$ m^2

that there are two constraints, geometric constraint (9) and straight posture of knee at heel strike, and hence, we choose $\boldsymbol{x} \in \mathbb{R}^3$ such as $\boldsymbol{x} = \left[\begin{array}{ccc} \theta_1 - \theta_2 - \theta_3 & \theta_4 & \theta_5 + \theta_6 \end{array} \right]^{\mathrm{T}}$.

Osuka et al. [12] chose the kinetic energy as observed value $\boldsymbol{y}(k)$. In this paper, we choose hip angle $\theta_1(k) - \theta_2(k)$ as an observed value, $y(k)$, where $\theta_1(k)$ is the support-leg angle and $\theta_2(k)$ is swing-leg angle of k-th heel strike. We note that $\theta_1(k) - \theta_2(k) = 2\theta_1(k)$ from geometric constraint and hence, only $\theta_1(k)$ is used as an observed value. For the simplicity, the DFC control input is assumed to be constant during a step. Then, hip torque is determined as

$$u_H(t) = c(\theta_1(k-1) - \theta_1(k-2)). \tag{21}$$

IV. SIMULATION RESULTS

In this section, we show simulation results of parametric excitation walking with and without DFC applied for a biped robot (Fig. 1), whose parameters are shown by Table I. We note that though it is not known a priori whether the condition, Eq. (19), is satisfied or not, we apply DFC to the parametric excitation walking. The condition, Eq. (19), will be checked only after an unstable equilibrium is found.

A. Suppression of bifurcation

First, we show that DFC input suppresses the two-period walking to one-period walking. We set the parameters of the reference trajectory as $A_m = 1.5$rad, $T_{\mathrm{set}} = 0.8$s and $\delta = 0.2$s. In two-period walking, high speed walking and low speed walking appear alternatively. In the simulation, we first generate parametric excitation walking without DFC hip torque, u_H. Once the gait converges to two-period walking, we apply DFC input u_H.

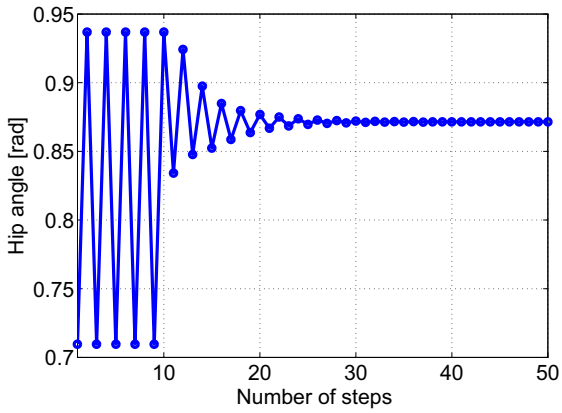

(a) Hip angle

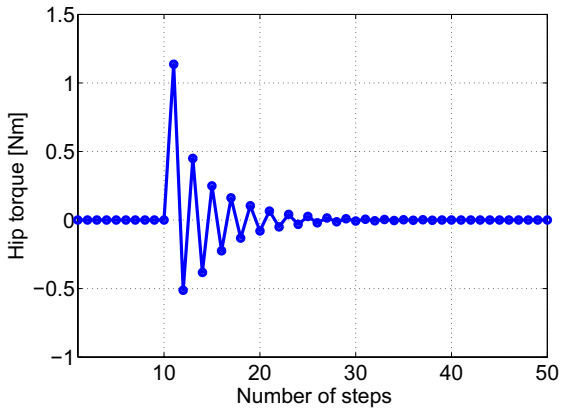

(b) Hip torque

Fig. 5. Effect of DFC

Fig. 5 illustrates the simulation results. Fig. 5(a) shows the hip angle $\theta_1 - \theta_2$ at heel strike and (b) shows the hip torque. Horizontal axis is the step number. From Fig. 5, it is observed that two-period walking is suppressed. Fig. 5(b) shows that hip torque given by Eq. (21) becomes zero as the gait converges to one-period walking.

B. Effect of DFC

In this subsection, we compare parametric excitation walking with and without DFC. Here, we apply DFC to both parametric excitation based forward bending walking and inverse bending walking.

Remark 4.1: In parametric excitation based inverse bending walking proposed by Harata et al. [9], swing-leg knee is bent in inverse direction to human. Regardless of bending direction, the center of mass of swing-leg moves up-and-down, and mechanical energy can be restored based on parametric excitation. We note that bifurcation also occurs in parametric excitation based inverse bending walking. □

Figs. 6 and 7 illustrate the simulation results of forward bending walking and inverse bending walking, respectively. Here, (a) is the step periods, (b) the walking speed and (c) the specific resistance. Specific resistance (SR) defined by

$$\mathrm{SR} = \frac{\int_{0^+}^{T^-} |u_K(\dot{\theta}_2 - \dot{\theta}_3)|\mathrm{d}t/T}{M_g g \overline{V}} \tag{22}$$

is used to evaluate energy efficiency. The smaller a specific resistance value is, the more efficient walking is. In Eq. (22), 0^+ and T^- represent the time just after and before collision at the ground, respectively, M_g is the total mass of a biped robot and $\overline{V}$ is the average walking speed of one step.

In Fig. 6 and 7, blue diamonds denote the results of parametric excitation method without DFC, red squares denote the average value of the results without DFC and green sold circles are the results of parametric excitation with DFC. In the case of two-period walking, there are two blue diamonds for each amplitude A_m, and their average value is shown by red square.

From Figs. 6 and 7, it is observed that all indices of the parametric excitation walking with DFC is better than the average values of the results without DFC. In particular, walking speed and specific resistance are improved significantly. SR without DFC varies nonsmoothly around the bifurcation point, while that with DFC varies smoothly.

C. Analysis using Poincaré map

In this subsection, we check the condition Eq. (19) numerically.

We use a Poincaré map which is used in evaluation of stability for walking cycle [13]. When we choose the Poincaré section as the instance just after heel strike, the mapping $\mathcal{F}$ in subsection III-B can be regard as Poincaré map.

In steady walking, the relation

$$\boldsymbol{x}^* = \mathcal{F}(\boldsymbol{x}^*, \boldsymbol{u}^*), \tag{23}$$

holds, where $\boldsymbol{x}^*$ is the stable state and u^* is the stable input, which is zero in our biped robot. The Poincaré map is stable if the absolute value of eigenvalues of matrix $\boldsymbol{A}$ defined by Eq. (18) are less than one. It is hard to derive matrix $\boldsymbol{A}$ analytically, so we compute its eigenvalues numerically.

The results are illustrated in Figs. 8 and 9. From Figs. 6 and 8, it is observed that bifurcation occurs when the absolute value of the maximum eigenvalue become larger than one. This is also holds for inverse bending walking (Figs. 7 and 9).

From these results show that two-period walking observed in parametric excitation walking is unstable periodic orbit, because the absolute value of maximum eigenvalue of $\boldsymbol{A}$ is larger than one. The results also show that the existence condition Eq. (19) of feedback gain is satisfied because the all eigenvalues are real and smaller than one.

V. CONCLUSION AND FUTURE WORK

In this paper, we proposed the method that stabilized walking in one period by combining the parametric excitation method with DFC. The proposed method designed the swing-leg knee torque by parametric excitation method and the hip torque by DFC. We numerically showed that walking performance of one-period walking with DFC was more efficient than that of two-period walking without DFC. In addition, we applied the proposed method to parametric excitation based inverse bending walking and then, the similar result was obtained. We also showed that the proposed method stabilizes unstable periodic orbit by using Poincaré map and then, the condition for applying DFC was satisfied.

In the future, we should show why bifurcation occurs and bifurcation exerts an adverse influence upon walking performance.

REFERENCES

[1] T. McGeer, "Passive dynamic walking," *Int. J. of Robotics Research*, vol. 9, no. 2, pp.62-82, 1990.

[2] A. Goswami, B. Espiau and A. Keramane, "Limit cycles in a passive compass gait biped and passivity-mimicking control laws," *J. of Autonomous Robots*, vol. 4, no. 3, pp. 273-286, 1997.

[3] F. Asano, M. Yamakita and K. Furuta, "Virtual passive dynamic walking and energy-based control laws," *Proceedings of the IEEE/RSJ Int. Conf. on Intelligent Robotics and Systems*, pp. 1149-1154, 2000.

[4] F. Asano, Z.W. Luo and S. Hyon, "Parametric excitation mechanisms for dynamic bipedal walking," *Proceedings of the IEEE Int. Conf. on Robotics and Automation*, pp. 611-617, 2005.

[5] F. Asano and Z.W. Luo, "Energy-efficient and high-speed dynamic biped locomotion based on principle of parametric excitation," *IEEE Trans. on Robotics*, vol. 24, no. 6 pp. 1289-1301, 2008.

[6] A. Goswami, B. Thuilot and B. Espiau, "A study of the passive gait of a compass-like biped robot: symmetry and chaos," *Int. J. of Robotics Research*, vol.17, no.12, pp. 1282-1301, 1998.

[7] K. Osuka and K. Kirihara , "Motion Analysis and Experiment of Passive Walking Robot Quartet II", *J. of Robotics Society of Japan*, vol. 18, no. 5, pp. 121-126, 2000 (in Japanese).

[8] Y. Harata, F. Asano, Z.W. Luo, K. Taji and Y. Uno, "Biped gait generation based on parametric excitation by knee-joint actuation," *Proceedings of the IEEE/RSJ Int. Conf. on Intelligent Robotics and Systems*, pp. 2198-2203, 2007.

[9] Y. Harata, F. Asano, K. Taji and Y. Uno, "Parametric excitation based gait generation for ornithoid walking," *Proceedings of the IEEE/RSJ Int. Conf. on Intelligent Robotics and Systems*, pp. 2940-2945, 2008.

[10] F. Asano and Z.W. Luo, "On efficiency and optimality of asymmetric dynamic bipedal gait," *Proceedings of the IEEE Int. Conf. on Robotics and Automation*, pp. 1972-1977, 2009.

[11] K. Pyrgas, "Continuous control of chaos by selfcontrolling feedback", *Physics Letters A*, vol. 170, pp. 421-428, 1992.

[12] K. Osuka, Y. Sugimoto and Toshiharu Sugie, "Stabilization of semi-passive dynamic walking based on delayed feedback control", *J. of Robotics Society of Japan*, vol. 22, no. 2, pp. 45-51, 2004 (in Japanese).

[13] A. Goswami, B. Thuilot, and B. Espiau, "Compass-like biped robot Part I: Stability and bifurcation of passive gaits", *INRIA Research Report*, no. 2996, October 1996.

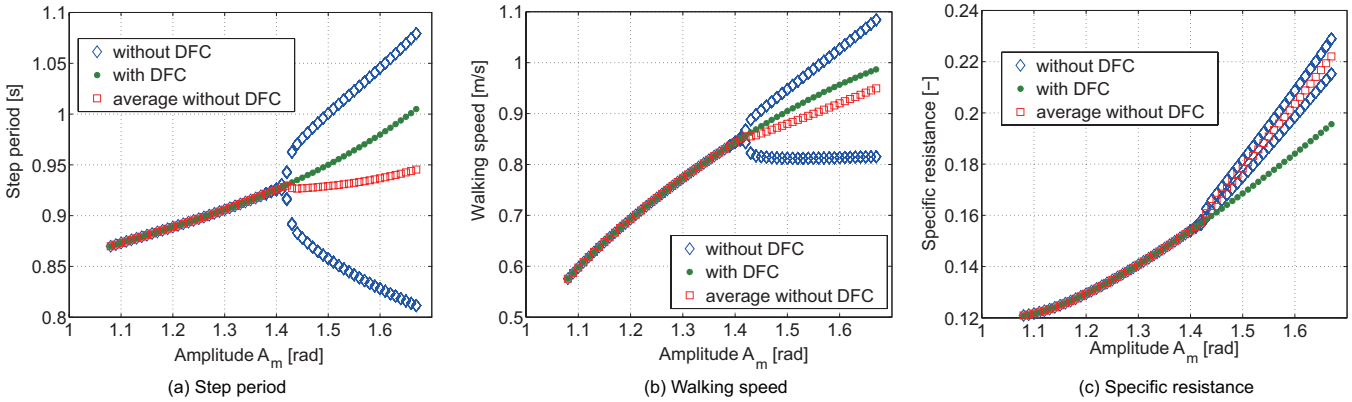

Fig. 6. DFC effect for forward bending walking with respect to A_m

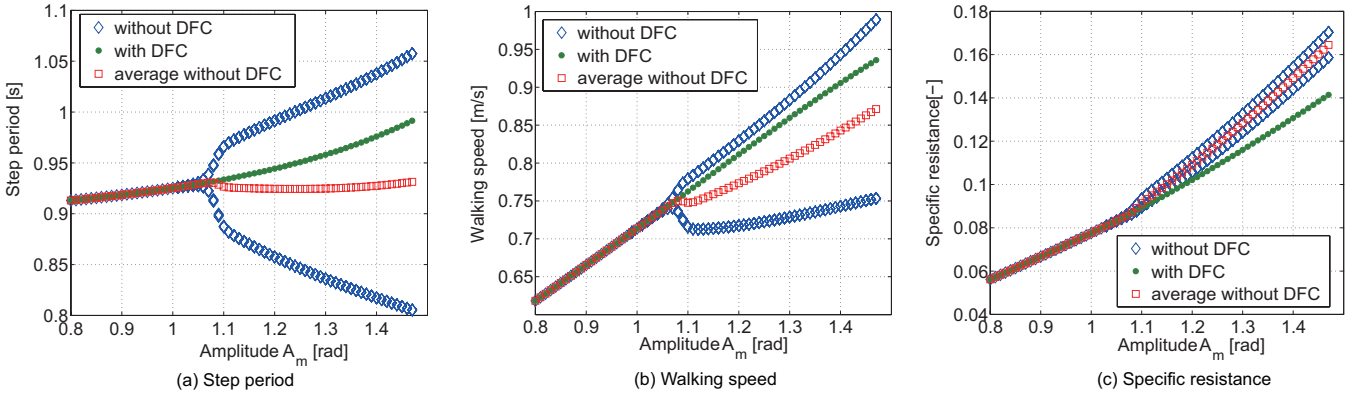

Fig. 7. DFC effect for inverse bending walking with respect to A_m

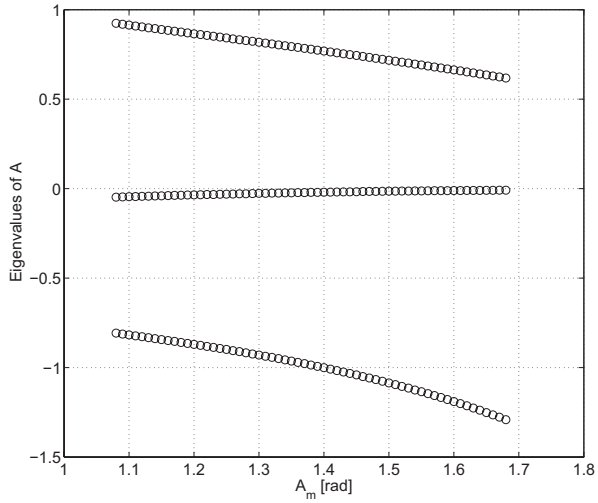

Fig. 8. Eigenvalues for forward bending walking

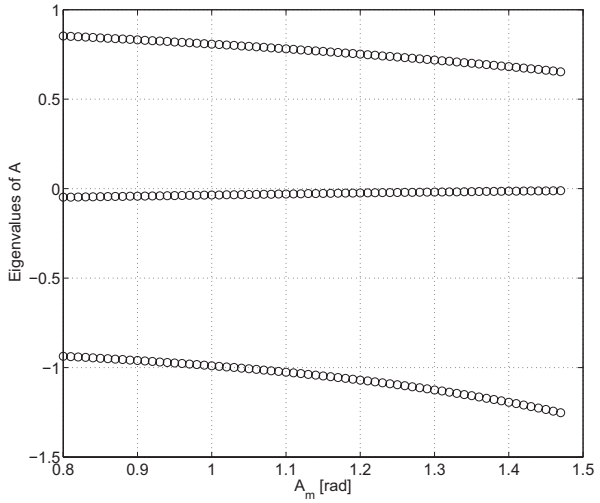

Fig. 9. Eigenvalues for inverse bending walking